5. ANKARA INTERNATIONAL AEROSPACE CONFERENCE **AIAC-2009-043**
17-19 August, 2009 - METU, Ankara - TURKEY

NUMERICAL INVESTIGATION OF FLOW CONTROL OVER AN AIRFOIL USING SYNTHETIC JETS AND ITS OPTIMIZATION

Eray Akçayöz[1] and İsmail H. Tuncer[2]
Middle East Technical University
Ankara, Turkey

ABSTRACT

The synthetic jet parameters for a NACA 0015 airfoil are optimized at various angles of attack to maximize the lift to drag ratio (L/D). Unsteady, turbulent flows are computed using a Navier-Stokes flow solver in a parallel computing environment. The Spalart-Allmaras turbulence model is employed in all computations. The Response Surface Methodology (RSM) is employed for the optimization of synthetic jet parameters; the jet velocity, the jet location, the jet angle and the jet frequency. The optimization study is performed for a constant value of jet power coefficient. The jet slot size is used as a dependent parameter in the optimization studies. The optimization study has shown that the jet velocity and the jet location are the dominant synthetic jet parameters. The optimum jet location is observed to be moving through the leading edge and the optimum synthetic jet angle is observed to be increasing as angle of attack increases for the separated flows. The flow separation on the suction side of the airfoil is observed to be delayed after the application of the synthetic jet. The L/D ratio is increased especially at the post stall angle of attacks. The effectiveness of the synthetic jet decreases for the attached flows.

INTRODUCTION

Flow control, either active or passive, aims to manipulate the flowfield over an aerodynamic body using various techniques [5]. The aim of the flow control can be to prevent/provoke separation, suppress/enhance turbulence or delay/advance transition to obtain benefits in the fields of L/D enhancement, drag reduction, lift enhancement, mixing augmentation and flow induced noise suppression [14]. In the active flow control, the flowfield is controlled by adding energy to the flow as opposed to the passive flow control. Using the active flow control, the lift coefficient can be increased without changing the angle of attack or deflecting the control surfaces.

The flow control devices working on the principle of steady suction or blowing and periodic suction or blowing are currently being investigated with applications in cars [3], helicopters [14], airplanes [11] and naval ships [4]. Suction or blowing type actuators require large amount of power, large space and they are mechanically complex, making them practically difficult to implement [8,12].

An effective active flow control device has been introduced recently which is called the synthetic jet. The synthetic jet is also called Zero Net Mass Flux (ZNMF) jet since it is created by oscillating the fluid around the airfoil periodically. The net mass flux is zero since the air surrounding jet orifice is sucked and blown periodically. The synthetic jet generates momentum difference that changes the behavior of the flow [1].

Figure 1 illustrates the sketch of a synthetic jet actuator. The fluid is drawn into and out of the cavity in the suction and blowing phases, respectively. The periodic suction and blowing motion of the air forms a vortex pair. As the vortex pair moves away from the orifice, the diaphragm sucks the fluid into the cavity and in the blowing phase, a new vortex pair is created. The generated vortex pairs interact with the separated flow region and causes low pressure region in the interaction zone. The low pressure

[1] Ph. D. Student in Aerospace Engineering Department, Email: eakcayoz@ae.metu.edu.tr
[2] Prof. in Aerospace Engineering Department, Email: tuncer@ae.metu.edu.tr

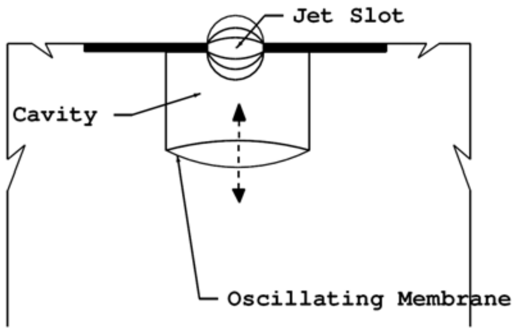

Figure 1: *Schematic representation of the synthetic jet actuator*

region around the synthetic jet causes partial or complete reattachment of the flow. Reattachment of the separated flow is responsible from the reduction in pressure drag [10].

The recent experimental and computational studies carried out for the flow control investigated the effect of synthetic jets on the flowfield over airfoils. However, the use of active flow control in the industrial aircraft design is still very limited.

An experimental study performed by Traub et al. [5] aims to evaluate the effectiveness of a synthetic jet actuator for the flow control on a pitching airfoil. The jet momentum coefficient and the slot exit width are the synthetic jet parameters varied. In all experiments, the airfoil was pitched from 0˚ to 27˚ at a constant angular velocity in 1 second. The results of the experiment have shown that the synthetic jet actuation delays the formation of the dynamic-stall-vortex to higher incidence angles.

Hamdani et al. [7] have studied the flow over NACA 0018 when alternating tangential blowing/suction is applied. The active flow control is found to be ineffective for the attached flows. The suction is found to be more effective than the blowing. It is observed that when the jet slot is located before 75% of the chord, the flow control becomes effective and the flow separation is suppressed. However, the flow control becomes ineffective when the slot is located at 0.75c which is at the downstream of the separation point.

A study performed by Martin et al. [9] aims to decrease helicopter pylon/fuselage drag using the active flow control. A thick airfoil, NACA 0036 is chosen as the baseline 2D test geometry. The separation point is observed to be much more severe at 10˚ than 0˚ angle of attack. The displacement thickness of the separated shear layer was reduced when the flow control is applied but still, a separated bubble is observed near the trailing edge. The flow control is reported to be more effective at 0˚ angle of attack case.

The synthetic jet recently has an application on Unmanned Air Vehicles, UAV. The synthetic jet concept over the wings of a UAV is applied by Parekh et al. [6]. It is reported that the turn rate was increased by controlling the leading edge separation and the weight of the flight control system was reduced. Another study performed by Patel et al. [8] for UAVs points out that the active flow control can be used in the development of UAVs without conventional control surfaces with a purpose of increasing maneuverability and reducing the weight.

The synthetic jet technology is used in a concept car named as Renault-Altica. The synthetic jet is located at the backside of the roof where the flow separates from the vehicle. A discreet mechanical system is used to generate air which is alternately blown and sucked through a 2mm wide slot. The drag is reduced by 15% at 130 km/h with an energy consumption of just 10 Watts by controlling the flow over the edge of the roof. The thickness of the separated flow region at the base of the car is reported to be decreasing when the synthetic jet is applied [3].

Donovan et al. [13] have investigated numerically the effect of the active flow control using steady and synthetic jets over NACA 0012 and NACA 0015 airfoils. Results of the Navier-Stokes computations using Spalart-Allmaras and SST turbulence models are compared with the experimental data. It is reported that both models show very good agreement before the stall, but deviate from the experimental data after the stall in the uncontrolled case. The computational results are not in exact agreement with the experiment for the controlled case, but the general trend is captured. In order to get same post-stall lift enhancement obtained with oscillatory jet, a steady jet with one to two orders of magnitude larger blowing momentum coefficient is required. For separated flow, the primary benefit of the actuator is reported to be reattachment of the separated flow partially. The studies over NACA 0012 airfoil showed that the actuators placed near the leading edge had a stronger effect than the actuators placed farther aft.

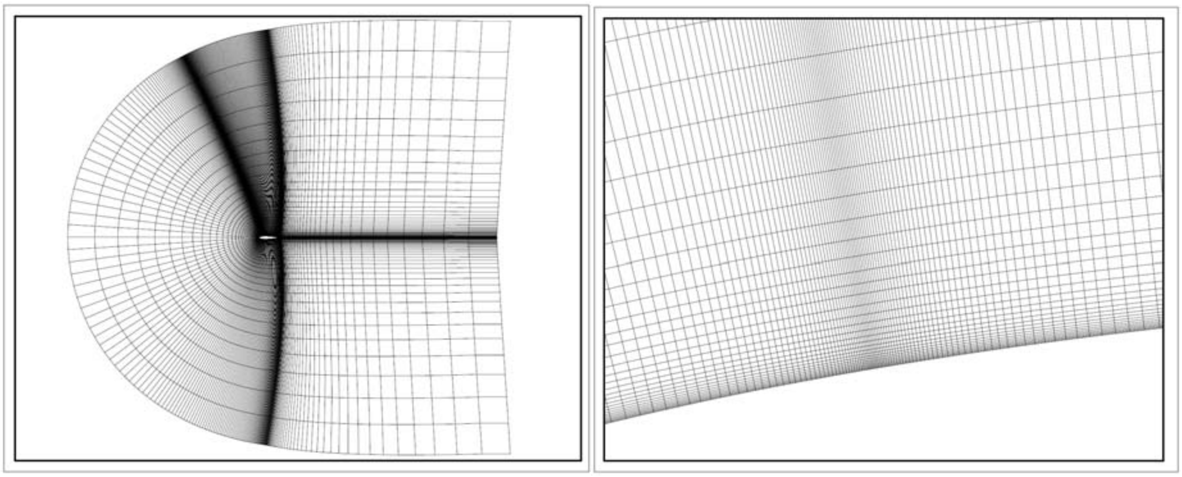

Figure 2: *A typical C-grid for NACA 0015 airfoil*

The Response Surface Methodology (RSM) is employed by Kaya et al. [2] for the optimization of periodically flapping airfoil parameters to maximize the thrust generation. The optimization using the RSM is found to be much more efficient than the optimization with the steepest ascent method. The RSM allows obtaining optimum parameters with similar accuracy by performing less number of computational evaluations.

In this study, the active flow control with a synthetic jet applied over a NACA 0015 airfoil is studied. The jet velocity, the jet frequency, the jet angle and the jet location are determined to be the optimization parameters. The jet slot size used as a dependent variable and all parameters are varied in a physically acceptable range such that the power coefficient of the synthetic jet is kept constant in each case. The RSM is used in the calculation of the optimum synthetic jet parameters. The optimization is carried out at three angles of attack values (α= 10˚, α= 14˚, α= 18˚) starting from pre-stall angle of attack and going up to post-stall angle of attack. The objective of the optimization is to determine synthetic jet parameters that maximize the lift to drag ratio.

METHOD

The numerical simulation of the active flow control is performed by a 2D Navier-Stokes flow solver. The unsteady flow calculations are performed at M=0.1, Re=8.96×10^5. The flow is assumed to be fully turbulent and one equation Spalart-Allmaras turbulence model is used. Computations are performed in parallel in a computer cluster. A structured, C-type grid is employed in the solution of flows around airfoil (Figure 2). The computational grid is refined at the synthetic jet location and at the leading and trailing edges.

The synthetic jet is introduced as a boundary condition at a specified location on the airfoil surface. The no-slip boundary condition applied on the airfoil surface is not valid at the synthetic jet location since a velocity vector is defined along the jet slot on the airfoil surface. The parameters used in the modeling of the synthetic jet are the non-dimensional jet velocity $(u_{jet}(s,t))$, non-dimensional jet location (x_{jet}), non-dimensional jet frequency (F_{jet}), non-dimensional jet slot size (L_{jet}) and jet angle (α_{jet}). A representative picture for the synthetic jet over the airfoil profile is shown in Figure 3.

The non-dimensionalization of the synthetic jet parameters are accomplished by the freestream speed of sound (a_∞) and airfoil chord length (c) as follows:

$$x_{jet} = \frac{x^*_{jet}}{c}, \quad L_{jet} = \frac{L^*_{jet}}{c}, \quad u_{jet} = \frac{u^*_{jet}}{a_\infty}, \quad F_{jet} = \frac{F^*_{jet} c}{a_\infty}$$

The jet momentum coefficient (C_μ) and the jet power coefficient (C_p) are defined as follows:

$$C_\mu = \rho_{jet} L_{jet} u_{jet}, \quad C_p = \rho_{jet} L^2_{jet} u^2_{jet} F_{jet}$$

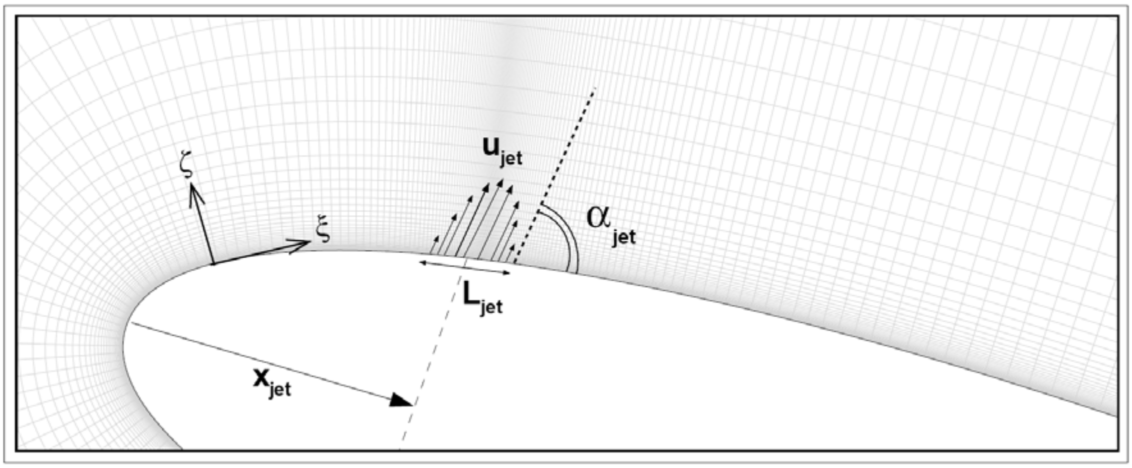

Figure 3: *The synthetic jet representation*

The Response Surface Methodology is employed in the optimization of the synthetic jet parameters. A quadratic response surface is approximated for L/D based on the Least Square method. The quadratic equation is the function of the jet velocity, the jet location, the jet angle and the jet frequency:

$$L/D = \beta_0 u_{jet}^2 + \beta_1 F_{jet}^2 + \beta_2 \alpha_{jet}^2 + \beta_3 x_{jet}^2 + \beta_4 u_{jet} F_{jet} + \beta_5 u_{jet} \alpha_{jet} + \beta_6 u_{jet} x_{jet} + \beta_7 F_{jet} \alpha_{jet} + \beta_8 F_{jet} x_{jet} + \beta_9 \alpha_{jet} x_{jet} + \beta_{10} u_{jet} + \beta_{11} F_{jet} + \beta_{12} \alpha_{jet} + \beta_{13} x_{jet} + \beta_{14}$$

where $\beta_0, \beta_1, ..., \beta_{14}$ are constant coefficients and L/D is the measured response.

The Box-Behnken (BB) and Full-Factorial (FF) Design of Experiment (DoE) techniques are employed to construct the optimization space. The optimization process is terminated if the relative error between the predicted and calculated responses is less than 1%.

The unsteady computations are carried out until a steady or a periodic behavior in aerodynamic coefficients is observed. The computed flowfields are analyzed in terms of pressure coefficient distribution, aerodynamic loads, wall shear stress and flowfields over the airfoil.

The optimization study is performed for a constant value of jet power coefficient $(C_p = 6 \times 10^{-7})$ which is the function of the density of air at the jet location, the jet velocity, the jet frequency and the jet slot size. In the computation of jet power coefficient, ρ_{jet} is assumed to be equal to the freestream density. The L/D is optimized by varying the synthetic jet parameters in a physically allowable range while keeping the value of the jet power coefficient constant. The jet slot size is calculated for each set of optimization variables therefore it is included to the optimization study as a dependent variable. The value of jet slot size observed to be changing between 0.15% and 0.9% of the chord. The jet location is changed between 10% and 90% of the chord length for all angles of attack values.

The design space for the optimization study is determined by considering the results of the parametric study together with the physical limitations of the synthetic jet. Table 1 summarizes the design space for the synthetic jet parameters employed in the optimization study.

Table 1: *Design space for the optimization study*

Variable	Minimum value	Maximum value
Jet velocity	0.1	0.3
Jet frequency	0.8	3
Jet angle	10	50
Jet location	0.1	0.9

Optimization case1: $\alpha = 10°$

The optimization study is carried out first at $\alpha = 10°$ which is a pre-stall angle of attack for the NACA 0015 airfoil. Convergence criterion is satisfied in 2 optimization steps as shown in Table 2. The optimization study is performed for 4 optimization variables then the jet velocity is excluded and 3 optimization variables are optimized in the second optimization step. The optimum jet location is estimated to be 10%c which is the most forward location in the optimization space. The absolute error in the L/D for the second optimization step is calculated to be 0.3%.

The response surfaces approximated at the second optimization step are shown in Figure 4. It is noted that the optimum L/D is estimated at the constraint boundary for the jet velocity, the jet frequency and the jet location with $\alpha_{jet} = 28.5°$.

Table 2: *Results of the optimization steps at* $\alpha = 10°$

Optimization Step	u_{jet}	F_{jet}	$\alpha_{jet}(°)$	x_{jet}	Estimated L/D	Calculated L/D	Error (%)
1	0.3	3.0	22.0	0.1	80.97	76.6	5.7
2	0.3	0.8	28.5	0.1	79.99	80.3	-0.3

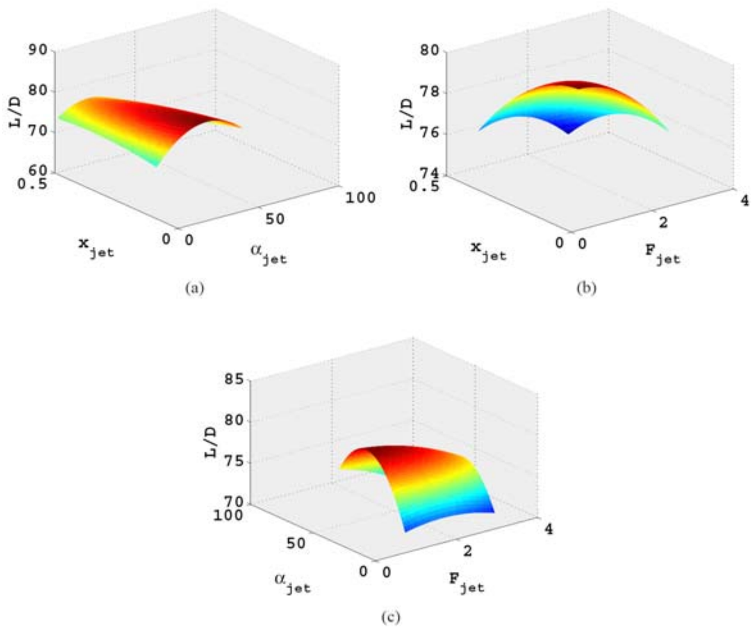

Figure 4: *Response surfaces at 2nd optimization step at* $\alpha = 10°$

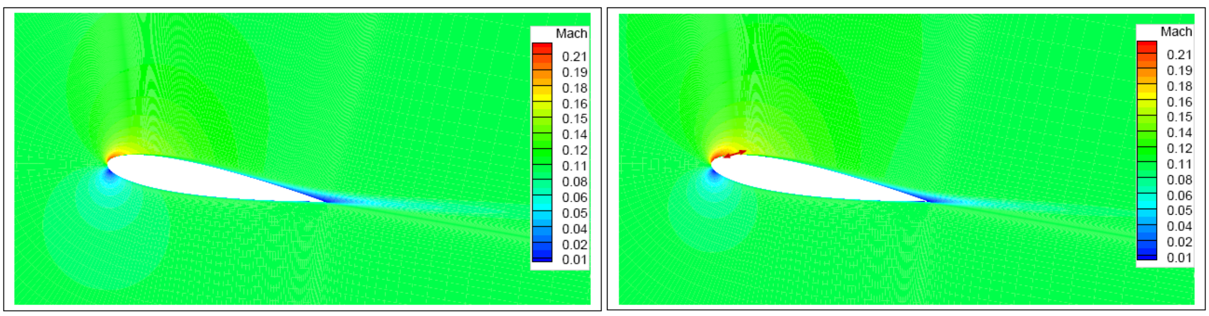

(a) No jet (b) With jet

Figure 5: *Average Mach contours at* $\alpha = 10°$

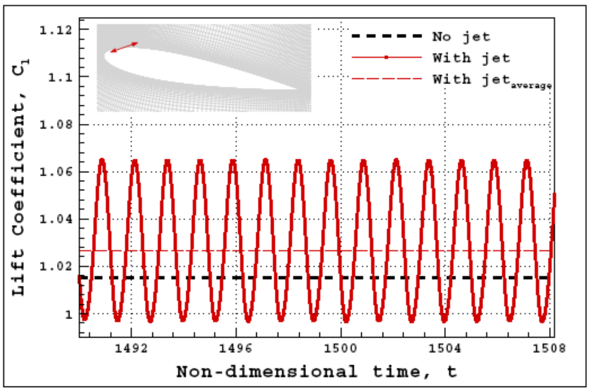

(a) Lift coefficient history

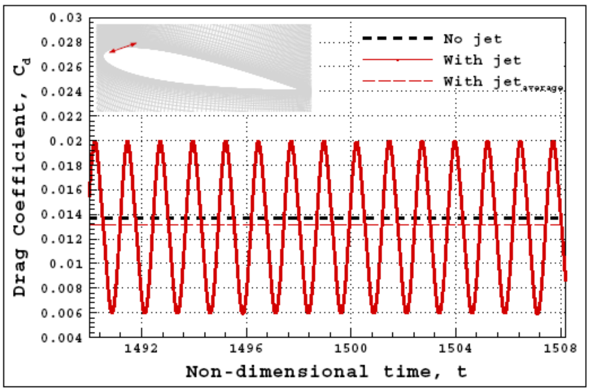

(b) Drag coefficient history

Figure 6: *Lift and drag coefficient histories at* $\alpha = 10°$

Table 2: *Aerodynamic coefficients at* $\alpha = 10°$

	C_l	C_d	L/D
No jet	1.01	0.0137	74.2
With jet	1.03	0.0128	80.3
Change(%)	1.5	-6.2	8.2

The average Mach contours are shown in Figure 5 for the cases before and after the application of the synthetic jet. The flow separation is observed through the trailing edge and the synthetic jet is observed to be almost ineffective on the separated flowfield around airfoil.

The variation of lift and drag coefficients in time is given in Figure 6. The variation in the lift and the drag coefficients after the synthetic jet application is observed to be relatively small. As given in Table 2, the reduction in the drag coefficient is observed to be 6.2% and the enhancement in the lift coefficient is observed to be 1.5%. The increase in the L/D is 8.2%.

Optimization case2: $\alpha = 14°$

The optimization study is next performed at $\alpha = 14°$. The results obtained through 3 optimizations steps are shown in Table 3.

Table 3: *Results of the optimization steps at* $\alpha = 14°$

Optimization Step	u_{jet}	F_{jet}	$\alpha_{jet}(°)$	x_{jet}	Estimated L/D	Calculated L/D	Error (%)
1	0.3	3.0	46.0	0.5	49.5	46.1	7.4
2	0.3	0.8	40.2	0.42	48.2	47.5	1.4
3	0.3	0.8	42.5	0.43	48.5	48.4	0.3

The response surfaces approximated at the third optimization step are shown in Figure 7. The optimum L/D is estimated when $\alpha_{jet} = 42.5°,\ x_{jet} = 0.42,\ F_{jet} = 0.8$.

Figure 8 shows the average Mach contours around airfoil before and after the synthetic jet application. It is observed that the vortex formed on the suction side of the airfoil reduces in size and moves towards the trailing edge after the application of the synthetic jet with the optimum parameters.

The variation of the lift and drag coefficients are shown in Figure 9. The variation of the lift and drag coefficients after the application of the synthetic jet are shown in Table 4. The reduction in the drag coefficient is observed to be 10.3% and the enhancement in the lift coefficient is observed to 5.6%. The L/D ratio is increased by 17.9%.

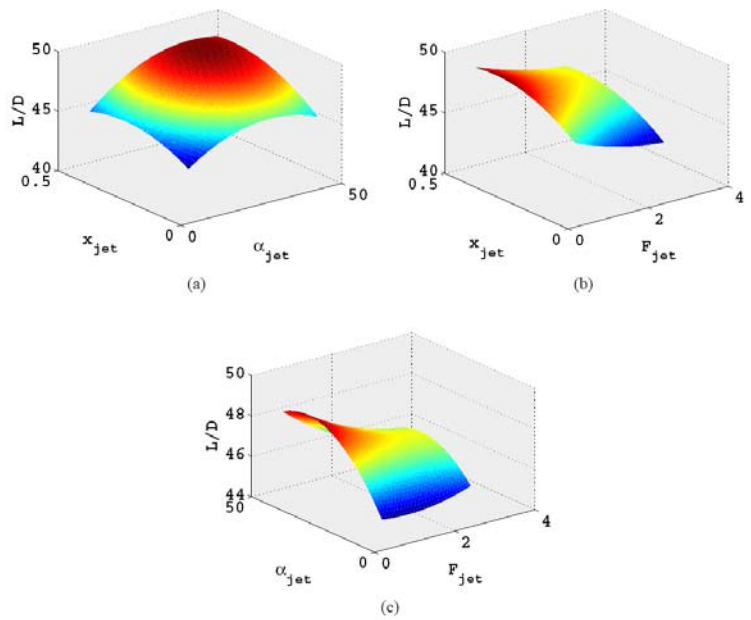

Figure 7: *Response surfaces at 2nd optimization step at* $\alpha = 14°$

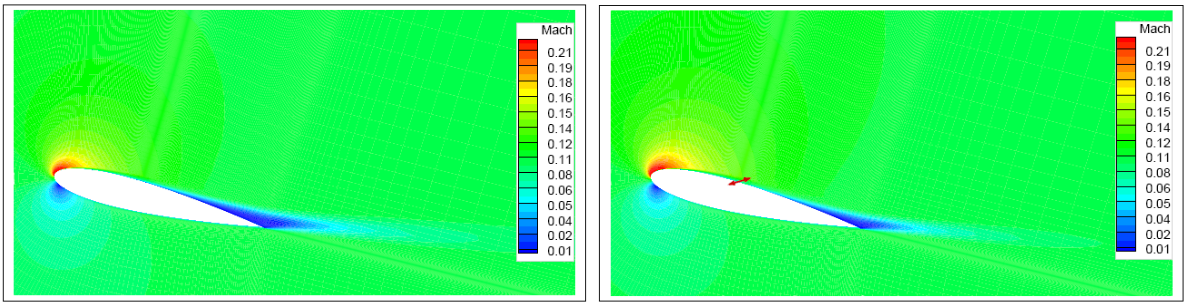

(a) No jet (b) With jet

Figure 8: *Average Mach contours at* $\alpha = 14°$

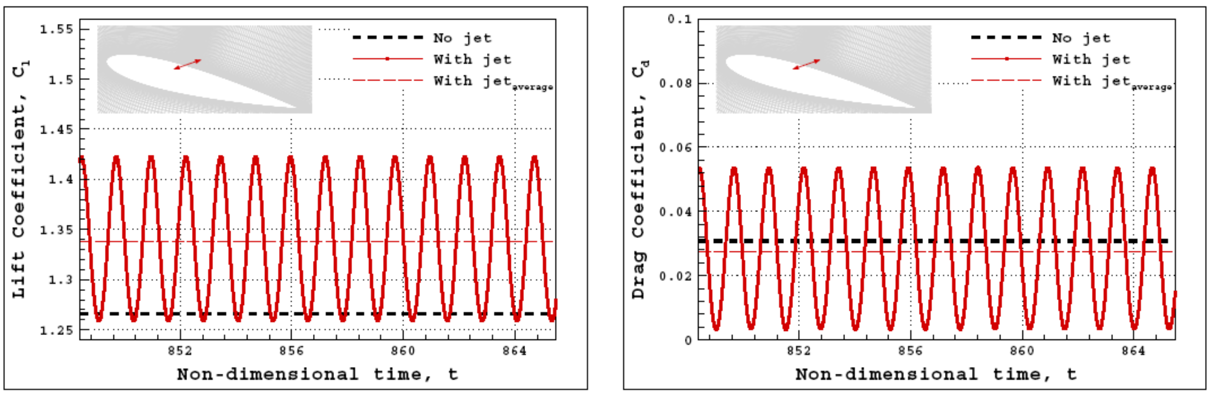

(a) Lift coefficient history (b) Drag coefficient history

Figure 9: *Lift and drag coefficient histories at* $\alpha = 14°$

Table 4: *Aerodynamic coefficients at* $\alpha = 14°$

	C_l	C_d	L/D
No jet	1.27	0.031	41.1
With jet	1.34	0.028	48.5
Change(%)	5.8	-10.3	17.9

Table 5: *Results of the optimization steps at* $\alpha = 18°$

Optimization Step	u_{jet}	F_{jet}	$\alpha_{jet}(°)$	x_{jet}	Estimated L/D	Calculated L/D	Error (%)
1	0.3	3.0	40.8	0.18	19.7	11.5	71.6
2	0.3	0.8	41.4	0.23	17.0	14.9	13.9
3	0.3	0.8	44.7	0.36	18.3	18.2	0.6

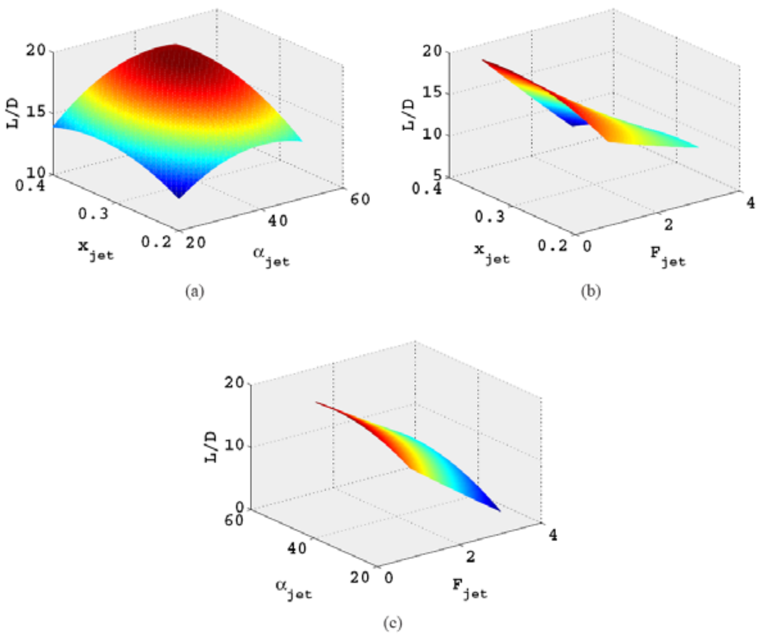

Figure 10: *Response surfaces at 2nd optimization step at* $\alpha = 18°$

Optimization case3: $\alpha = 18°$

The optimization study is finally performed at $\alpha = 18°$ which is a post stall angle of attack for the NACA 0015 airfoil. The optimization process is terminated in 3 optimization steps. Table 5 shows the values of the optimum design parameters and relative errors obtained in optimization steps.

The RSM surfaces approximated for 3 optimization variables (when $u_{jet} = 0.3$) at the final optimization step are shown in Figure 10. The RSM surfaces illustrates that the maximum L/D is obtained when $\alpha_{jet} = 44.7°, x_{jet} = 0.36, F_{jet} = 0.8$.

The average Mach contours around the airfoil before and after the application of the synthetic jet are shown in Figure 11. The vortex formed on the suction side of the airfoil is observed to be significantly reduced in size and the flow separation moves towards the trailing edge.

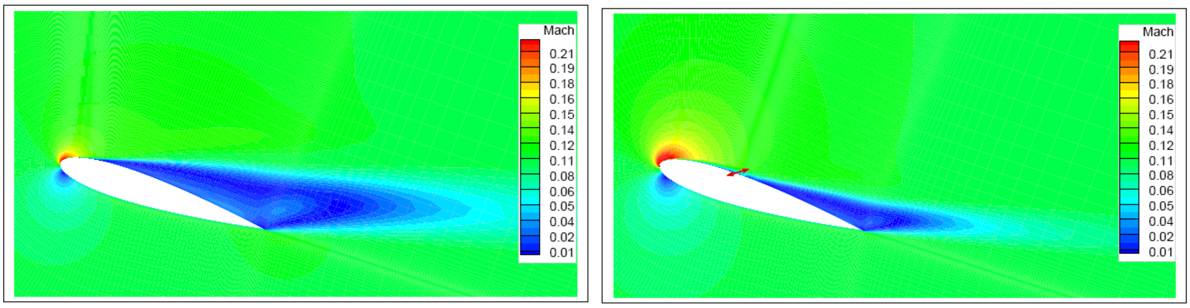

(a) No jet (b) With jet

Figure 11: *Average Mach contours at* $\alpha = 18°$

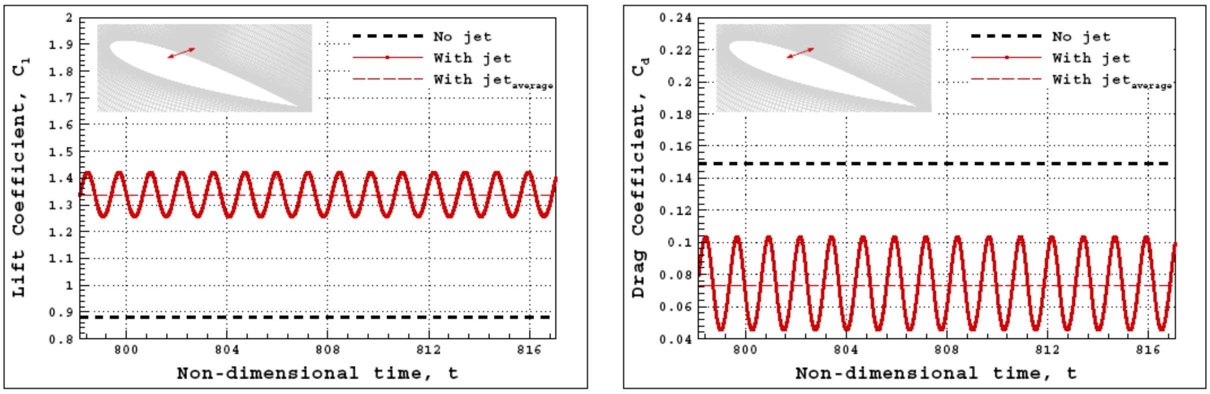

(a) Lift coefficient history (b) Drag coefficient history

Figure 12: *Lift and drag coefficient histories at* $\alpha = 18°$

Table 6: *Aerodynamic coefficients at* $\alpha = 18°$

	C_l	C_d	L/D
No jet	0.87	0.15	5.9
With jet	1.33	0.077	18.2
Change(%)	52.6	-51.0	211

The variation of lift and drag coefficients are shown in Figure 12. Both the lift and the drag coefficients are observed to be oscillating at a constant amplitude and frequency when synthetic jet is applied. The frequency of oscillations and frequency of the synthetic jet are observed to be the same. The application of the synthetic jet increases the average lift coefficient by 52.6% and reduces the average drag coefficient by 51% which corresponds to 211% increase in the L/D when compared with the no jet case as given in Table 6.

The variations of the lift and drag coefficients, the L/D ratio and the point of separation with angle of attack are summarized in Figure 13. It is seen in Figure 13 (a) that the lift coefficient increases when the synthetic jet is applied with the optimal parameters. The stall angle of attack is also delayed with the synthetic jet actuation. The variation of drag coefficient with angle of attack is shown in Figure 13 (b). It is observed that drag coefficient is reduced significantly at $\alpha = 18°$. The L/D variation shown in Figure 13 (c) reveals that the L/D curve also shifts upward with the synthetic jet actuation. The location of the separation point with varying angle of attack before and after the synthetic jet application is given in Figure 13 (d). It is noted that the application of the synthetic jet delays the flow separation at all angles of attack. The synthetic jet is observed to be least effective at $\alpha = 10°$ where the flow is mostly attached.

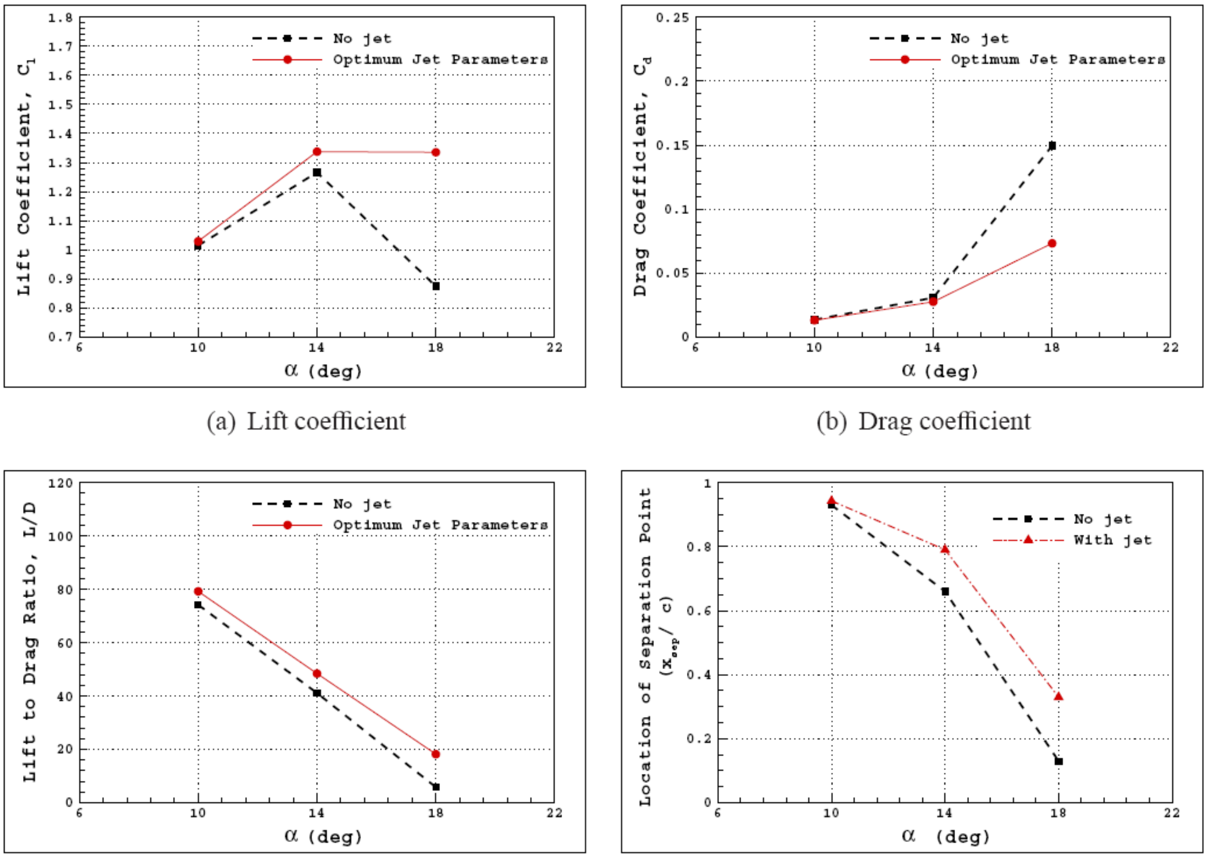

(a) Lift coefficient (b) Drag coefficient

(c) L/D (d) Separation point location

Figure 13: *Results of the optimization study*

CONCLUSIONS

The numerical simulation of active flow control with synthetic jets is successfully studied for flows over airfoil sections. Unsteady flow solutions are obtained by a 2D Navier-Stokes flow solver. The flow is assumed to be fully turbulent and one equation Spalart-Allmaras turbulence model is used. Computations are performed in parallel in a computer cluster. The synthetic jet parameters are then optimized at various angles of attack to maximize the L/D ratio using the Response Surface Methodology. The computational results are investigated by examining the instantaneous and the phase averaged flowfields, the aerodynamic load variations in time and the separation point location. The optimization study shows that the synthetic jet is the most effective at post-stall angles of attack. It enhances the L/D ratio significantly and delays the flow separation for separated flows. The optimum synthetic jet velocity is always observed to be the maximum value in the design space at all angles of attack. The optimum synthetic jet angle is observed to be increasing as the angle of attack increases. The optimum synthetic jet location and the location of separation point are observed to be moving through the leading edge as the angle of attack increases from 14˚ to 18˚. A smaller jet frequency corresponds to a larger jet slot size for a constant jet power coefficient, and the optimum synthetic jet frequency is observed to be the minimum value in the design space at all angles of attack

References

[1] Akçayöz, E., *Numerical Investigation of Flow Control Over an Airfoil with Synthetic Jets and its Optimization*, M.S. Thesis, Middle East Technical University, 2008.

[2] Kaya, M. and Tuncer, İ. H., *Response Surface Method for the Maximization of Thrust in Flapping Airfoils*, AIAC-2007-011," 4th Ankara International Aerospace Conference, 2007.

[3] Renault, *Renault Altica: 44MPG Diesel Concept with Active Airflow Management*, 2006, http://www.greencarcongress.com/2006/02/renault altica .html.

[4] Kitsios, V., Kotapati, R., Mittal, R., Ooi, A., Soria, J., and You, D., *Numerical Simulation*

of Lift Enhancement on a NACA 0015 Airfoil Using ZNMF Jets, Proceedings of the Summer Program, 2006, pp. 457.

[5] Traub, L., Miller, A., and Rediniotis, O., *Effects of Synthetic Jet Actuation on a Ramping NACA 0015 Airfoil*, Journal of Aircraft, Vol. 41, No. 5, 2004, pp. 1153–1162.

[6] Parekh, D., Glezer, A., Allen, M., Crittenden, T., and Birdsell, E., *AVIA: Adaptive Virtual Aerosurface*, Defense Technical Information Center, 2004.

[7] Hamdani, H., Baig, A., and Zahir, S., *A Systematic Study of Separation Control by Varying Various Parameters During Alternating Tangential Blowing/Suction*, AIAA paper, Vol. 422, 2003.

[8] Patel, M., Kolacinski, R., Prince, T., Ng, T., and Cain, A., *Flow Control Using Intelligent Control Modules for Virtual Aerodynamic Shaping*, AIAA Paper, Vol. 3663, 2003.

[9] Martin, P., Tung, C., Chandrasekhara, M., and Arad, E., *Active Separation Control: Measurements and Computations for a NACA 0036 Airfoil*, 21st AIAA Applied Aerodynamics Conference, 2003.

[10] Vadillo, J., *Numerical Study of Virtual Aerodynamic Shape Modification of an Airfoil Using a Synthetic Jet Actuator,* Ph.D. thesis, Washington University, 2002.

[11] Gad-el Hak, M., *Flow Control: The Future*, Journal of Aircraft, Vol. 38, No. 3, 2001, pp. 401.

[12] Mallinson, S., Hong, G., and Reizes, J. A., *Fundamental Studies of a Synthetic Jet Actuator*, University of Technology Sydney, 13th Australian Fluid Mechanics Conference, 1998.

[13] Donovan, J., Krai, L., and Cary, A., *Active Flow Control Applied to an Airfoil*, AIAA Paper no, 1998, pp. 98–0210.

[14] Gad-el Hak, M., *Modern Developments in Flow Control*, Appl. Mech. Rev, Vol. 49, No. 7, 1996, pp. 365–379.